3772–3786 Nucleic Acids Research, 2013, Vol. 41, No. 6 Published online 7 February 2013
doi:10.1093/nar/gkt059

Co-regulated expression of alpha and beta mRNAs encoding HLA-DR surface heterodimers is mediated by the MHCII RNA operon

Laura Pisapia[1], Valeria Cicatiello[1,*], Pasquale Barba[1], Donatella Malanga[2], Antonella Maffei[1,3], Russell S. Hamilton[4] and Giovanna Del Pozzo[1]

[1]Institute of Genetics and Biophysics 'Adriano Buzzati Traverso'—CNR, Naples, 80131, Italy, [2]Department of Experimental and Clinical Medicine, Magna Graecia University of Catanzaro, University Campus Germaneto, Catanzaro 88100, Italy, [3]Department of Medicine of Columbia University Medical Center, New York 10032, NY, USA and [4]Department of Biochemistry, University of Oxford, OX1 3QU Oxford, UK

Received August 28, 2012; Revised January 14, 2013; Accepted January 15, 2013

ABSTRACT

Major histocompatibility complex class II (MHCII) molecules are heterodimeric surface proteins involved in the presentation of exogenous antigens during the adaptive immune response. We demonstrate the existence of a fine level of regulation, coupling the transcription and processing of mRNAs encoding α and β chains of MHCII molecules, mediated through binding of their Untraslated Regions (UTRs) to the same ribonucleoproteic complex (RNP). We propose a dynamic model, in the context of the 'MHCII RNA operon' in which the increasing levels of DRA and DRB mRNAs are docked by the RNP acting as a bridge between 5′- and 3′-UTR of the same messenger, building a loop structure and, at the same time, joining the two chains, thanks to shared common predicted secondary structure motifs. According to cell needs, as during immune surveillance, this RNP machinery guarantees a balanced synthesis of DRA and DRB mRNAs and a consequent balanced surface expression of the heterodimer.

INTRODUCTION

Major histocompatibility complex class II molecules (MHCII) are cell-surface glycoproteins that play a pivotal and essential role in the regulation of the adaptive immune response, as they induce development, activation and survival of CD4 T cells, through presentation of extracellular antigens (1).

MHCII are expressed by different cell types named antigen-presenting cells (APCs), which are distinguished into two major categories on the basis of their potential for antigen presentation: professional or non-professional. Professional APCs are cells of haematopoietic origin specialized in the priming of naïve T cells and include dendritic cells, B lymphocytes and cells of monocyte/macrophage lineage (2). Non-professional APCs are non–bone marrow-derived cells that constitutively express MHCII molecules but do not have a complete range of co-stimulatory molecules, such as thymic epithelial cells (3) and endothelial cells in various organs, as well as cell types that do not have basal levels of MHCII molecules but can be induced in response to interferon-γ (4). This category also includes tumour cells from several solid neoplastic tissues, where it is not surprising to find CD4 T helper lymphocytes specific against tumour antigens MHCII-restricted. The level of expression of MHCII molecules on the surface of APCs is strictly related to the functioning of the immune response in infection, transplantation, cancer and autoimmunity (5).

MHCII genes encode the polymorphic human leucocyte antigens (HLA): HLA-DR, HLA-DQ and HLA-DP proteins, present as α and β heterodimers on the cell surface, and their expression is mainly regulated at the level of transcription by a highly conserved regulatory module site in the promoters of the genes in all vertebrate species. Four key *trans*-acting factors, constitutively expressed, bind these modules while the cell-specific, cytokine-induced and developmentally regulated expression of MHCII genes is ensured by Class II Transactivator (CIITA), the master key transcriptional activator that mediates its function not through a direct binding to DNA but through interaction with the proteins of enhanceosome (6). This complex machinery guarantees a coordinated transcriptional regulation of all MHCII genes; so far no data are available for post-transcriptional events. Recent evidence from our laboratory

*To whom correspondence should be addressed. Tel: +39 0816132309; Fax: +39 0816132718; Email: cicatiello@igb.cnr.it

The authors wish it to be known that, in their opinion, the first two authors should be regarded as joint First Authors.

demonstrated that mRNAs encoding DR and DQ isotypes are assembled in the cytoplasm in a functional unit defined 'MHCII RNA operon' in which the 3′-UTRs of different transcripts bind the same ribonucleoproteic complex (RNP), among which we have identified two proteins: ErbB3 Binding Protein 1 (EBP1) and Nuclear Factor 90 (NF90) (7). Both factors are well characterized RNA-binding proteins that can influence mRNA in terms of stability and translation (8,9) and can also act on the transcriptional expression of the same gene (10,11).

In this work, by interfering with the physiological equilibrium between DRA and DRB transcripts, we found that the ectopic expression of one mRNA influences the transcription of the other endogenous mRNA. We investigated the stoichiometric balance between messengers encoding α and β chains and the maintenance of the equilibrium, already established with transcription, to determine whether this mechanism is preserved during all steps of mRNA processing up to the surface expression of proteins. We found that a coordinated modulation occurs and is mediated through the presence of 5′- and 3′-UTR signals that physically bind proteins of the RNA operon.

MATERIALS AND METHODS

Reagents, cell lines and flow cytometry analysis

M14 and Raji, a human melanoma and a human B lymphoma cell line, respectively, were cultured in RPMI 1640 medium, whereas HeLa, a human epithelial cell line, was cultured in Dulbecco's modified Eagle's medium, both media supplemented with 10% Foetal Calf Serum (FCS). Primary monocytes were prepared from buffy-coat of a healthy donor. The peripheral blood mononuclear cells recovered by centrifugation over Ficoll Paque Plus (Amersham Biosciences) gradient were further purified by a multistep Percoll gradient, obtaining a monocyte 80% pure population, as assessed by flow cytometry with an anti-CD14 antibody (data not shown). To measure the mRNA half-life, actinomycin D (Act D) (10 μg/ml) was added to cell cultures after 48 h from transfection for 2, 4 and 6 h.

Determination of cell surface expression of MHCII antigens was performed by cytofluorimetric analysis using the FACSAria cell-sorting system and analysed by the DIVA software (BD Biosciences). Fluorescein isothiocyanate (FITC) mouse anti-human HLA-DR and CD14, along with the appropriate FITC mouse IgG isotype control, were purchased from BD Biosciences.

Transfections

All plasmids used were prepared by cloning cDNAs in pSVK3 expression vector and are represented in Supplementary Table S1 and described in Supplementary Methods.

Silencing of EBP1 and NF90 was performed with siRNAs and procedures previously described (7), and transfection of p5DRA3 and p5DRB3 was carried out 24 h after silencing. For mRNA recovery, cells were harvested at 6, 18 and 42 h after transfection (corresponding to 30, 48 and 72 h from the beginning of the experiment, respectively).

M14 stable transfectants were carried out by transfection of CMV10-3× FLAG vector containing cDNA encoding EBP1 p48 isoform, kindly provided by Prof A. Hamburger (12).

Chromatin immunoprecipitation

Chromatin immunoprecipitation (ChIP) assay was performed as described previously (13), with several modifications reported in Supplementary Methods. In all, 1.5×10^6 M14 cells were transfected with 4 μg of pSVK3, p5DRB3 and p5DRBΔ, and the cells were harvested after 48 h. The pre-cleared chromatin was immunoprecipitated with 5 μg of anti-RNA Pol II C-terminal repeat domain P-S5 antibody (Abcam). One-tenth of the immunoprecipitated DNA and input DNA were analysed by quantitative reverse transcriptase–polymerase chain reaction (qRT–PCR) using DRA-c-F and DRA-c-R promoter primers (Supplementary Table S2).

All Ct values were normalized to their own input and are expressed as $2^{\Delta\Delta Ct}$ between sample immunoprecipitated with anti-PolII and with rabbit anti-IgG (14). The values obtained were further normalized to pSVK3, considered equal to one.

RNA quantization and riboprobes synthesis

For the isolation of total RNA, after lysis of cells in QIAzol Lysis Reagent (QIAGEN), the total RNA was purified using phenol–chloroform extraction. All RT reactions were performed using the QuantiTect RT Kit (QIAGEN). Nucleus–cytoplasmic RNA preparation was carried out 48 h after transfection by PARIS kit from AMBION. The amount of specific transcripts was measured by qRT–PCR, through the DNA Engine Opticon Real-Time PCR Detection System (BIORAD), using the amount of cDNA obtained retro-transcribing 0.5 μg of total RNA. The QuantiTect SYBR Green PCR Kit (QIAGEN) was used to perform all the reactions in presence of 0.2 μM primers (Supplementary Table S2), synthesized by PRIMM; each assay was run in triplicate.

All DNA fragments used for the riboprobes synthesis were prepared as previously described (7) or were obtained by PCR, using full-length cDNAs as template and the primers indicated in Supplementary Table S2. The transcription reactions were performed to obtain cold biotin-conjugated CTP and [^{32}P] UTP-labelled riboprobes using T7 *in vitro* transcription system MAXIScript T7 (Ambion). 5DRA, 5DRB, 3DRA and 3DRB templates are the 5′- and 3′-UTRs of the corresponding cDNAs, synthesized by primers listed in Supplementary Table S2. 5DRAΔ and 5DRBΔ templates were obtained by enzyme digestion of 5DRA construct with AvaI and 5DRB construct with BsmAI (see sequences in Supplementary Data). Ubiquitin-conjiugated enzyme (UBC) template negative control corresponds to 122 nt of the 3′-UTR.

Pull-down and 5′–3′ co-precipitation assays

In all, 120 μg of cytoplasmic proteins were incubated for 30 min at room temperature with 1 μg of biotinylated transcripts in TENT-binding buffer (10 mM Tris–HCl pH 8, 1 mM ethylenediaminetetraacetic acid, pH 8, 250 mM NaCl, 0.5% v/v Triton X-100). RNPs were isolated with streptavidin-conjugated Dynabeads (Invitrogen); beads were washed three times with TENT, and proteins were separated by sodium dodecyl sulphate polyacrylamide gel electrophoresis (SDS–PAGE). The presence of NF90 protein was verified by western blot analysis with specific anti-DRBP76 (anti-double stranded RNA binding protein 76 or anti-NF90) antibody (BD Biosciences), whereas the presence of EBP1 protein was confirmed by anti-FLAG-M2 (Sigma) and anti-EBP1 (Abcam) antibodies.

To carry out 5′–3′ co-precipitation assay, 300 ng of biotinylated RNA was bound to 2 μl of streptavidin-conjugated Dynabeads for 60 min at room temperature in the following buffer: 14 mM HEPES, pH 7.5, 6 mM Tris–HCl, pH 7.5, 60 mM KCl, 1 mM dithiothreitol, 1 mM ethylenediaminetetraacetic acid and 1 U RNase OUT. The ^{32}P-labelled RNA (~10 ng) was incubated with bovine serum albumin (BSA) or with increasing amount of rEBP1 or rNF90 (0, 0.1, 0.2, 0.4, 0.8 and 1 μg), in presence of 1 U of RNase OUT and 1 μg of yeast tRNA, or 30 min at room temperature. The reaction mixtures were combined and incubated for additional 40 min. The beads were collected by centrifugation and washed with buffer containing 50 mM Tris–HCl, pH7.5, 300 mM KCl, 1 mM MgCl2 and 0.05% NP40. The RNA was released from the beads and analysed on a 7 M urea and 6% Tris/Borate/EDTA acrylamide gel (15). The radioactive images were acquired by Typhoon analysis (Amersham Bioscience).

Computational search for common motifs

To determine whether there are common stem–loops between the 5′- and 3′-UTRs of HLA-DRA (ENSG00000228987) and HLA-DRB (ENST00000360004), a Foldalign analysis was performed. The Foldalign algorithm simultaneously folds and aligns pairs of RNA sequences to give either local or global structural alignments (16). Significant local alignments for motifs common between the sequences were then filtered; hence, only alignments with >50% sequence identity were included. The RNA-binding proteins NF90 and EBP1 contain sequence/structure-specific domains; therefore, there is a likely requirement for sequence as well as structural similarity between motifs.

Statistical analysis

All results shown are the mean of three independent experiments. Statistical analysis was performed using the unpaired Student's *t*-test with two-tailed distribution and two sample equal variance parameter. In the figures, asterisk corresponds to $P < 0.05$ and double asterisk corresponds to $P < 0.01$.

RESULTS

Ectopic expression of cDNA encoding a single α or β chain modulates the level of MHCII surface heterodimer

Plasmids pSVK3, p5DRA3, p5DRAΔ, pΔDRA3, pΔDRAΔ, p5DRB3 and p5DRBΔ (Supplementary Table S1) were transiently transfected into M14 melanoma cell line that constitutively expresses low levels of MHCII molecules, and the variation of surface expression of HLA-DR heterodimers was measured after 48 h by fluorescence-activated cell sorting analysis. Surprisingly, we observed (Figure 1A) that after transfection of a single full-length DRA or DRB cDNA, the surface expression of entire DR heterodimer is increased by ~2-fold if compared with cells transfected with pSVK3 empty control ($P < 0.05$ and $P < 0.01$, respectively). We did not observe this phenomenon when we transfected DRA or DRB cDNAs 5′- and/or 3′-UTR deleted, indicating an involvement of these regions in the modulation of HLA-DR surface expression (Figure 1A).

To assess whether the surface increase of DR molecule corresponds to an equal one of mRNA synthesis, we also looked at the variations of HLA-DRA and HLA-DRB transcripts by qRT–PCR. At 48 h from transfection of the full-length p5DRA3, we observed a 14-fold increase in the amount of HLA-DRA mRNA and a relative 13-fold augmentation of the endogenous HLA-DRB mRNA. The same result was obtained when we transfected p5DRB3 (Figure 1B). In contrast, after p5DRAΔ pΔDRA3 and pΔDRAΔ transfections (Figure 1B), the analysis revealed 2- to 3-fold increase for both DRA and endogenous DRB mRNAs; this phenomenon is also observed after p5DRBΔ transfection. Taken together, these results give several indications for the existence of co-regulation between the two chains: we have observed an endogenous increase of a chain dependent on the amount of the other chain ectopically expressed. This phenomenon is absent or only weakly underlined when both or at least one of the regulatory 5′- or 3′- UTRs are lacking. The contemporary presence of 5′- and 3′-UTRs flanking the coding region of DRA or DRB is able to induce a strong increase of its own mRNA and an unequivocal co-regulation of the related chain.

In Supplementary Figure S1, we showed the kinetics of mRNA variation until 72 h after transfection for each constructs, in which it seems evident that the increase of endogenous messengers is consequent to that of the exogenous transcription with a little time delay.

To clarify the involvement of 5′- and 3′-UTRs, we generated chimeric constructs in which the DRA coding region has been replaced with the green fluorescent protein (GFP) cDNA (see Supplementary Table S1). Forty-eight hours after M14 transfection, we confirmed the GFP expression by microscopy (data not shown), and we measured the amount of GFP, DRA and DRB mRNAs by qRT–PCR (Figure 1C and D) to discriminate the endogenous synthesis of mRNA. We observed that the plasmid p5GFP3 carrying both DRA UTRs is able to induce a 5- and 6-fold increase of DRA and DRB mRNAs, respectively, whereas the constructs p5GFPΔ and pΔGFP3 lacking one of these regulatory regions induce a 2- to 3-fold increase of the same

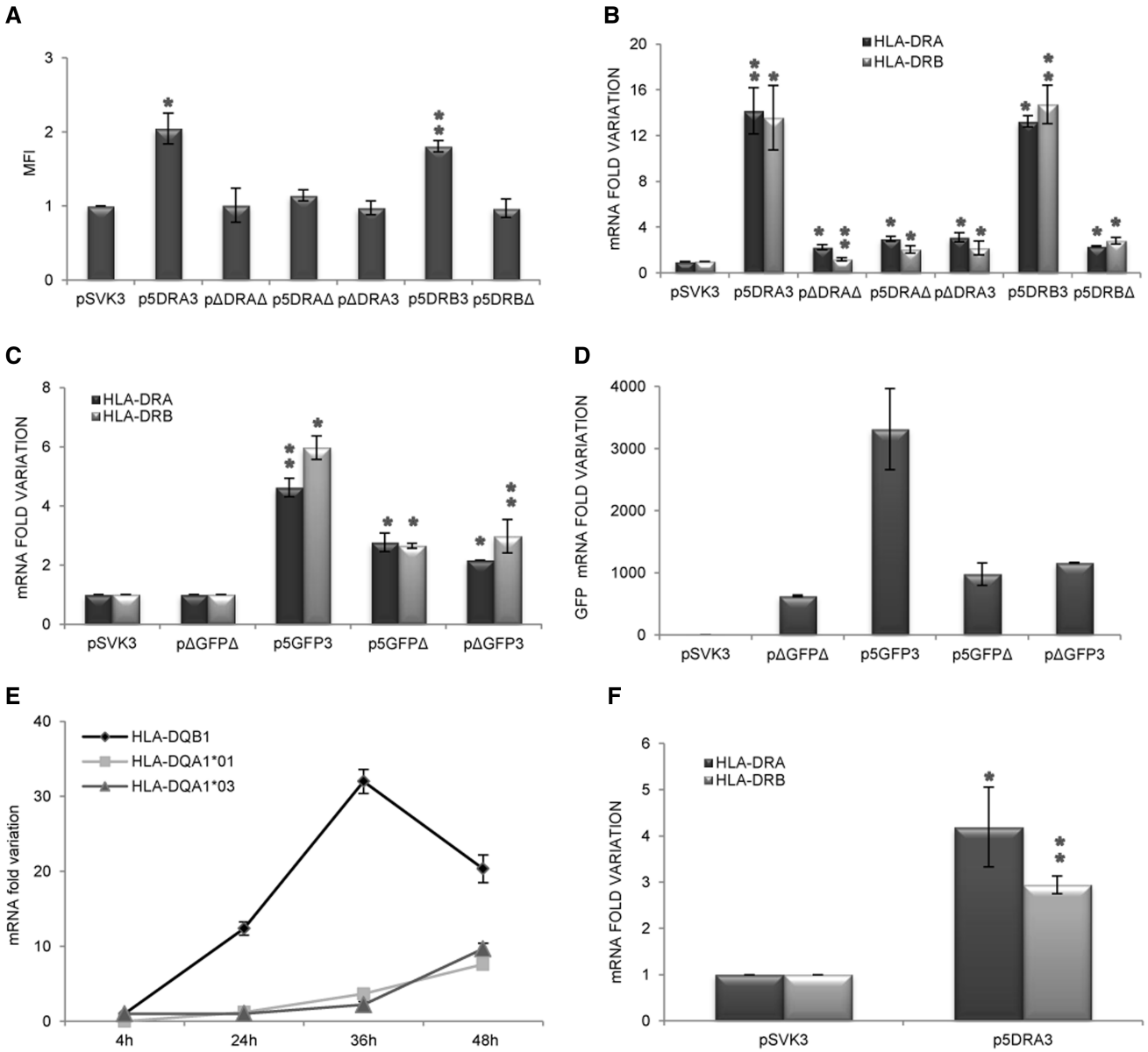

Figure 1. Quantitative analysis of MHCII expression during co-regulation. (**A**) Cytofluorimetric analysis of HLA-DR surface expression: M14 cells are stained with HLA-DR FITC-conjugated–specific antibody 48 h after transfection with indicated plasmids. Results are plotted as fold change of MFI. (**B**) Quantification of DRA and DRB mRNAs by qRT–PCR of cells transfected in the same experimental conditions. mRNA amount is plotted as fold change. *P*-value is relative to pSVK3. qRT–PCR analysis of DRA and DRB mRNAs (**C**) and GFP mRNA (**D**) at 48 h after transfection of M14 with pSVK3, pΔGFPΔ, p5GFP3, p5GFPΔ and pΔGFP3. Results are plotted as fold change compared with pSVK3, and *P*-value is relative to pΔGFPΔ. (**E**) Quantification of HLA-DQB and HLA-DQA1*01 and HLA-DQA1*03 mRNAs alleles by qRT–PCR after transfection of M14 with p5DQB3 construct. The graph shows fold variation with respect to pSVK3 at 4, 24, 36 and 48 h. (**F**) Quantification of DRA and DRB mRNAs by qRT–PCR in primary monocytes cells 6 h after nucleofection with pSVK3 and p5DRA3 plasmids. The graph shows DRA and DRB mRNA fold variation, and *P*-value is compared with the control.

endogenous and exogenous mRNAs. When we transfected pΔGFPΔ, we did not observe any variation. At the same time, the presence of both 5′- and 3′-UTRs flanking the GFP cDNA induced an increase of its mRNA amount, compared with the expression of plasmid containing only GFP cDNA (Figure 1D); the presence of one of the regulatory regions 5′- or 3′-UTRs showed an intermediate profile. The use of chimeric plasmid p5GFP3 confirmed that the phenomenon of co-regulation is dependent on the presence of both 5′- and 3′-UTR regions that seem to act in a synergistic way, as in presence of only one UTR, we observe a partial effect. We can affirm that these regulatory regions are able to induce an mRNA increase by *de novo* transcription or stability increase of the messengers.

To establish whether the co-regulated expression of two mRNAs is a general mechanism valid for all isotypes of MHCII molecules, we transfected M14 with p5DQB3 construct carrying the cDNA of HLA-DQB1 gene and its 5′- and 3′-UTR control regions. We harvested cells at different time points and measured HLA-DQB1 and both

HLA-DQA1*01 and HLA-DQA1*03 mRNAs by qRT–PCR (Figure 1E); 36 h after transfection, we observed 30-fold increase of DQB mRNA and 16-fold increase of the DQA1 mRNA expressed by two alleles (*01 and *03). In conclusion, also for DQ isotype, the ectopic expression of the messenger encoding one chain increases the endogenous mRNA amount encoding the other chain.

Furthermore, we demonstrated that the co-regulated expression of two mRNAs encoding the heterodimeric MHCII molecule is a general mechanism also occurring in professional APCs. We nucleofected p5DRA3 construct in Raji B lymphoma cell line and carried out a time course analysis of mRNAs encoding α and β chain by qRT–PCR. As observed in M14, we also appreciated in Raji cells an upregulation of DRB mRNA (Supplementary Figure S2). In addition, *ex vivo* primary monocytes prepared from a blood sample of a healthy donor were transfected by nucleofection with p5DRA3, and cells were harvested 6 h afterwards for measurement of DRA and DRB mRNAs (Figure 1F). The graph shows 4-fold increase of DRA mRNA, derived from both transfected and endogenous cDNAs, and a linked 2.5-fold change of endogenous DRB mRNA ($P < 0.05$ and $P < 0.01$, respectively).

Our data support, for the first time, the existence of a mechanism in which the expression of a heterodimeric protein, derived by the translation of two independent transcripts, is regulated through the reciprocal balance of these transcripts. This co-regulation, highlighted in professional and non-professional *in vitro* APC and in *ex vivo* monocytes, can involve transcriptional and post-transcriptional events.

The MHC II mRNAs co-regulation occurs through transcriptional and post-transcriptional events

To assess the contribution of the transcription to the co-regulation mechanism, we have analysed whether the increase of the endogenous mRNA after transfection is caused by a greater activity of PolII on the MHCII promoter. To address this, we transfected M14 cell line with p5DRB3 and p5DRBΔ plasmids, and, 48 h afterwards, we performed a ChIP assay with an anti-RNA PolII antibody to analyse the transcriptional activity on endogenous DRA promoter, in such a manner to determine the endogenous α DRA mRNA synthesis. In Figure 2A, we reported the fold occupancy by PolII on DRA promoter after transfection of two constructs compared with empty pSVK3 plasmid. We found that, after transfection by p5DRB3 construct, there is an increase of α chain endogenous transcription of ~0.5 with respect to the control ($P < 0.05$), but we did not observe any variation when we transfected the 3′-UTR–deleted plasmid. When an mRNA coding for a single MHCII chain is overexpressed, the cells reach a balance in the amount of both messengers through a transcriptional increase of the other related gene; this mechanism is possible only if the mRNA has an intact 3′-UTR.

To unravel the events occurring at a post-transcriptional level, we investigated the nucleus–cytoplasm export of two messengers encoding for the same isotype. We transfected M14 cells with full-length and deleted constructs, and we monitored the variation in the mRNA content in cytoplasmic versus nuclear fractions at 48 h after transfections. The results are shown in Figure 2B as a cytoplasmic/nuclear (C/N) ratio. This ratio is established equal to 1 after transfection with p5DRA3 construct, increasing to almost 2 when we transfected p5DRAΔ or pΔDRA3 (statistically significant versus p5DRA3) and to 4.5 when both UTRs are absent (pΔDRAΔ transfection, $P < 0.01$) without significant differences between DRA and DRB mRNAs. Similar differences are shown in Figure 2C for the other transcript, comparing the ratio obtained for p5DRB3 and p5DRBΔ ($P < 0.05$); export of β-actin mRNA remained unchanged (data not shown). The trend of the ratio indicates that the export rate of two messengers is balanced and coordinated, and the UTRs influence the speed of transport out of nucleus, according to data previously published (17).

Furthermore, we evaluated the kinetics of mRNA decay in cells transfected for 48 h with p5DRA3 and p5DRB3, whose transcription we have blocked with Act D treatment for 2, 4 and 6 h. Total mRNA was analysed for DRA and DRB by qRT–PCR, and results were normalized to the β-actin mRNA levels and expressed as percentage of maximum. First, we calculated ($T_{1/2} = \mathrm{Ln}(0.5)/\mathrm{slope}$) the half-lives of endogenous mRNAs in cells transfected with empty vector pSVK3 (Figure 3A), and we found that DRA mRNA ($t_{1/2} = 3.24$ h) was more stable than DRB mRNA ($t_{1/2} = 2.6$ h). Next we analysed the steady-state of mRNAs in cells transfected with full-length constructs, and we found that after p5DRA3 ectopic expression (Figure 3B), there was a significant half-life increase of both DRA ($t_{1/2} = 3.92$ h) and endogenous DRB ($t_{1/2} = 3.19$ h) mRNAs, compared with those of cells transfected with pSVK3 ($P < 0.05$ and $P < 0.01$, respectively). Similarly after p5DRB3 transfection (Figure 3C), we found an analogous half-life increase of endogenous DRA ($t_{1/2} = 4.02$ h) and DRB ($t_{1/2} = 3.41$ h) transcripts, compared with the control ($P < 0.05$ and $P < 0.01$, respectively). In conclusion, the ectopic expression of a full-length mRNA encoding α or β chain induces stability increase of the proper and of the mRNA encoding the cognate chain, indicating a coordinated regulation of the decay of the two mRNAs.

We also measured the half-life of GFP after transfection of chimeric plasmids. Using pΔGFPΔ, we measured $t_{1/2} = 1.9$ h (Figure 3D); after p5GFP3 transfection, there was an evident increase of its half-life ($t_{1/2} = 3.71$ h), whereas the presence of only one regulatory region 5′- or 3′-UTR showed an intermediate profile, with $t_{1/2} = 2.86$ and 2.77 for p5GFPΔ and pΔGFP3, respectively. GFP mRNA with both UTRs is more stable with respect to GFP mRNA lacking these sequences. Finally, (Figure 3E), we reported the half-life of endogenous DRB mRNA after GFP chimeric constructs transfection. When we transfected pΔGFPΔ, we measured $t_{1/2} = 2.58$ h of DRB mRNA, equal to half-life assessed in control cells; after the expression of constructs with only one regulatory region, p5GFPΔ and pΔGFP3,

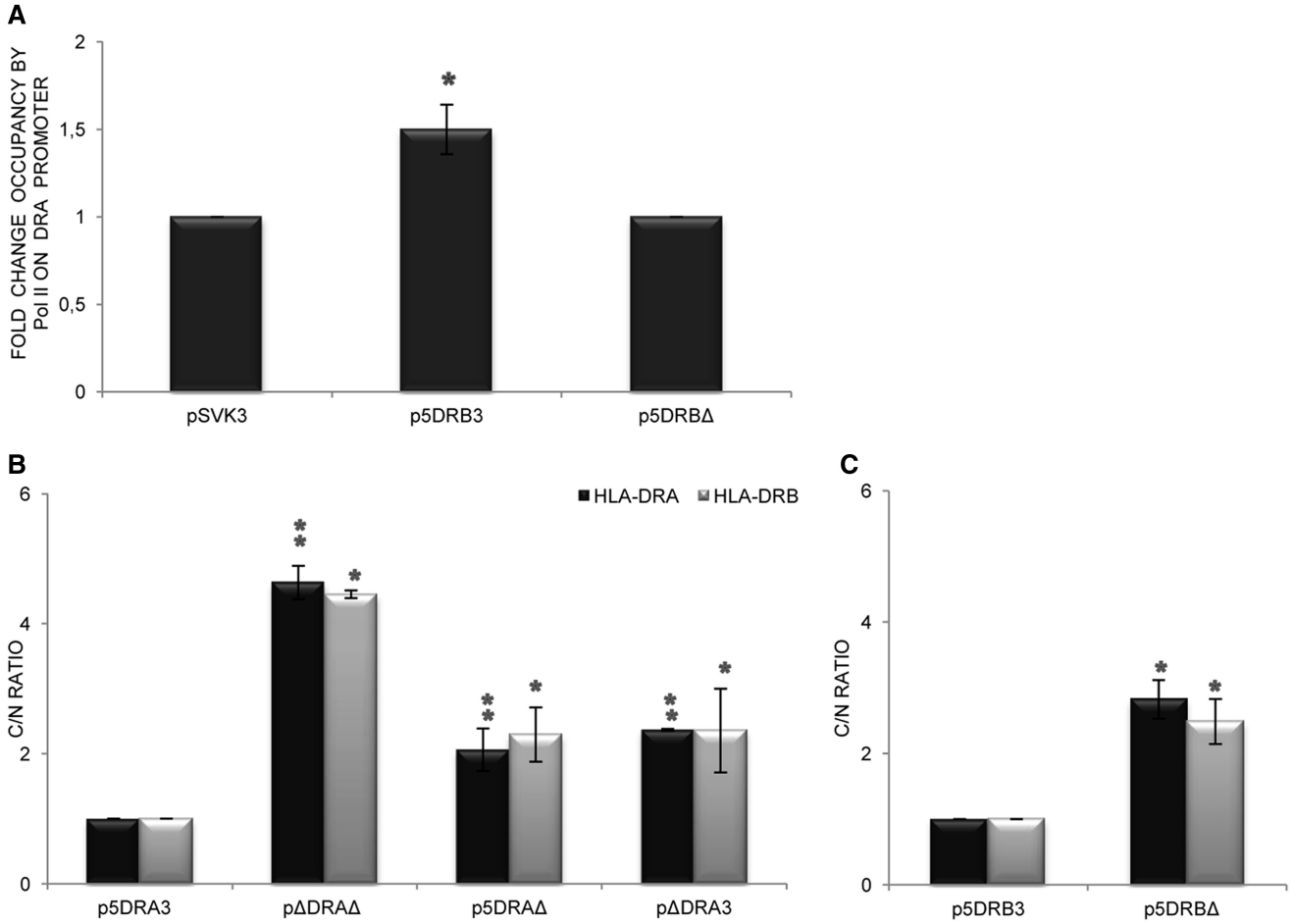

Figure 2. ChIP assay and nucleus–cytoplasm export during MHC II mRNA co-regulation. (**A**) HLA-DRA promoter occupancy by PolII was analysed by ChIP assay in M14 cells at 48 h from transfection with full-length p5DRB3 or p5DRBΔ-deleted constructs. The histograms represent the fold variation compared with pSVK3, which indicates the basal rate of DRA transcription. *P*-value is related to pSVK3. (**B**) and (**C**) Quantification by qRT–PCR of cytoplasmic and nuclear DRA and DRB mRNAs in M14 cells at 48 h after transfection with indicated plasmids. Results are plotted as cytoplasm/nucleus (C/N) mRNA ratio in two compartments, and *P*-value is related to p5DRA3 (B) or p5DRB3 (C), which we consider equal to 1.

the DRB half-life increased to $t_{1/2} = 3$ and to $t_{1/2} = 2.89$ h, respectively. p5GFP3 transfection showed a strong half-life increase of endogenous DRB mRNA ($t_{1/2} = 3.46$ h), similar to results obtained transfecting p5DRA3 (3B). These data indicate that the presence of UTR sequences stabilizes both MHCII transcripts and no related messenger.

In conclusion, our experiments indicate that after the ectopic expression of full-length MHCII cDNA encoding one chain, there is an augment of mRNAs half-lives of the endogenous transcript encoding for the other chain, indicating a coordinate modulation of stability and an '*in trans*' effect. Moreover, we have observed an '*in cis*' effect of UTRs regulatory regions on the modulation of endogenous DRA and DRB genes expression.

The depletion of EBP1 and NF90 influences DRA and DRB mRNAs expression

In a previous article (7), we demonstrated that the specific silencing of EBP1 (Figure 4A-I) and NF90 (Figure 4A-II) induces the downregulation of both DRA and DRB mRNAs. To assess the contribution of EBP1 and NF90 proteins to the co-regulation of α and β chains, we performed EBP1 and NF90 knockdown experiments followed by transfections of p5DRA3 or p5DRB3 constructs, and we monitored DRA and DRB mRNAs variation by qRT–PCR. After 24 h of silencing with siCtlr, siEBP1 and siNF90, we transfected p5DRA3 or p5DRB3 constructs, and cells were harvested for mRNA quantification at 6, 18 and 42 h of plasmid transfection (corresponding to 30, 48 and 72 h from the beginning of the experiment).

We established that EBP1 and NF90 silencing inhibits the overexpression of ectopic mRNAs (p5DRA3 in A-V and A-VII, p5DRB3 in A-VI and A-VIII), and consequently that of endogenous mRNAs compared with siCtlr (A-III and A-IV). Either EBP1 or NF90 silencing inhibits the co-regulation mechanism blocking mRNA increase, induced by transfection, avoiding the mechanism of co-regulated expression of DRA and DRB transcripts.

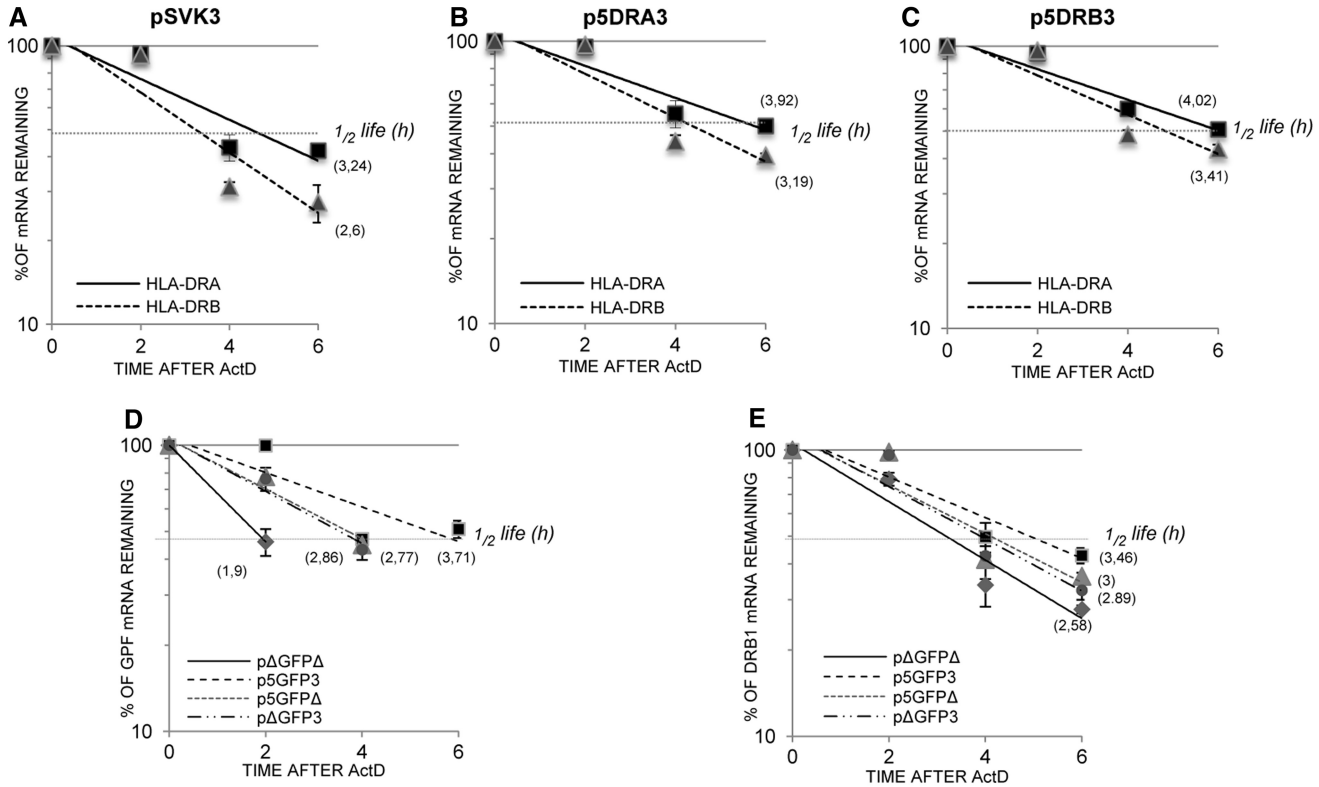

Figure 3. DRA and DRB mRNA half-lives during co-regulation. Kinetics of DRA and DRB mRNAs decay in M14 cells assessed 48 h after pSVK3 (**A**), p5DRA3 (**B**) and p5DRB3 (**C**) transfections. The cells were harvested after 2, 4 and 6 h of Act D treatment, and the percentages of remaining mRNAs are showed. Kinetics of GFP (**D**) and DRB (**E**) mRNA decay in M14 cells assessed 48 h after p5GFP3, p5GFPΔ, pΔGFP3 and pΔGFPΔ transfections. The cells were harvested after 2, 4 and 6 h of Act D treatment, and the percentages of remaining mRNAs are showed. The half-life of mRNAs, shown in parentheses, was calculated with the following formula $T_{1/2} = \mathrm{Ln}(0.5)/\mathrm{slope}$, indicating the required time for a given transcript to decrease to 50% of its initial abundance.

Relative contribution of DRA and DRB messengers to MHCII density

We tested the relative DRA and DRB mRNAs contribution to the MHCII heterodimer density in HeLa cell line in which the MHCII molecules are not constitutively expressed. We transiently transfected p5DRA3 and p5DRB3 in HeLa cells, maintaining a fixed amount of one chain while changing the amount of the other and evaluated the modulation of DR surface expression, represented as mean fluorescence intensity (MFI) fold variation in B-I of Figure 4. In particular, using a constant amount of p5DRA3 (3 μg) and a variable amount of p5DRB3 (3, 2 and 1 μg), we measured a decreasing HLA-DR surface density. When we used a constant amount of p5DRB3 (3 μg) and a variable amount of p5DRA3 (3, 2 and 1 μg), we appreciated a more rapid and significant MFI decrease than that observed when we scale down p5DRB3 ($P < 0.05$). Then we looked at differences in the DRA and DRB total mRNAs and observed (Figure 4B-II) that both mRNAs varied in a coordinated manner, according to the smallest amount of messenger, even with excess of the other. In addition we noted that, in both protein and mRNA expression, there are different kinetics, in that the transfection with decreasing p5DRA3 amount determines a more rapid and significant reduction of HLA-DRB mRNA ($P < 0.01$) compared with the transfection carried out with decreasing p5DRB3 amount that determines a slower and not significant variation of HLA-DRA mRNA. In other words, the expression of DRA mRNA has a prevalent role in the establishment of a stoichiometric ratio between the two transcripts and provides a major contribution to the determination of heterodimer density. This modulation could be due to the higher stability of DRA compared with DRB, as reported in the previous experiment, probably a consequence of a different interaction with proteins of the operon.

5′-UTRs take part in the RNP complex

We have previously demonstrated that DRA and DRB mRNAs, such as DQA mRNA, are included in a ribonucleoproteic complex, in which 3′-UTRs of MHCII messengers bind to EBP1 and NF90 proteins, among other not yet identified proteins (7). To investigate the involvement of 5′-UTR of DRA and DRB transcripts in the RNP complex, we first performed RNA-Electrophoretic mobility shift assay (REMSA) using cytoplasmic protein extracts. We have designed two riboprobes, corresponding to 5′-UTR sequences upstream of the ATG initiation codon of DRA and DRB mRNAs, named 5DRA and 5DRB, respectively (see Supplementary Table S3 for sequences). REMSAs

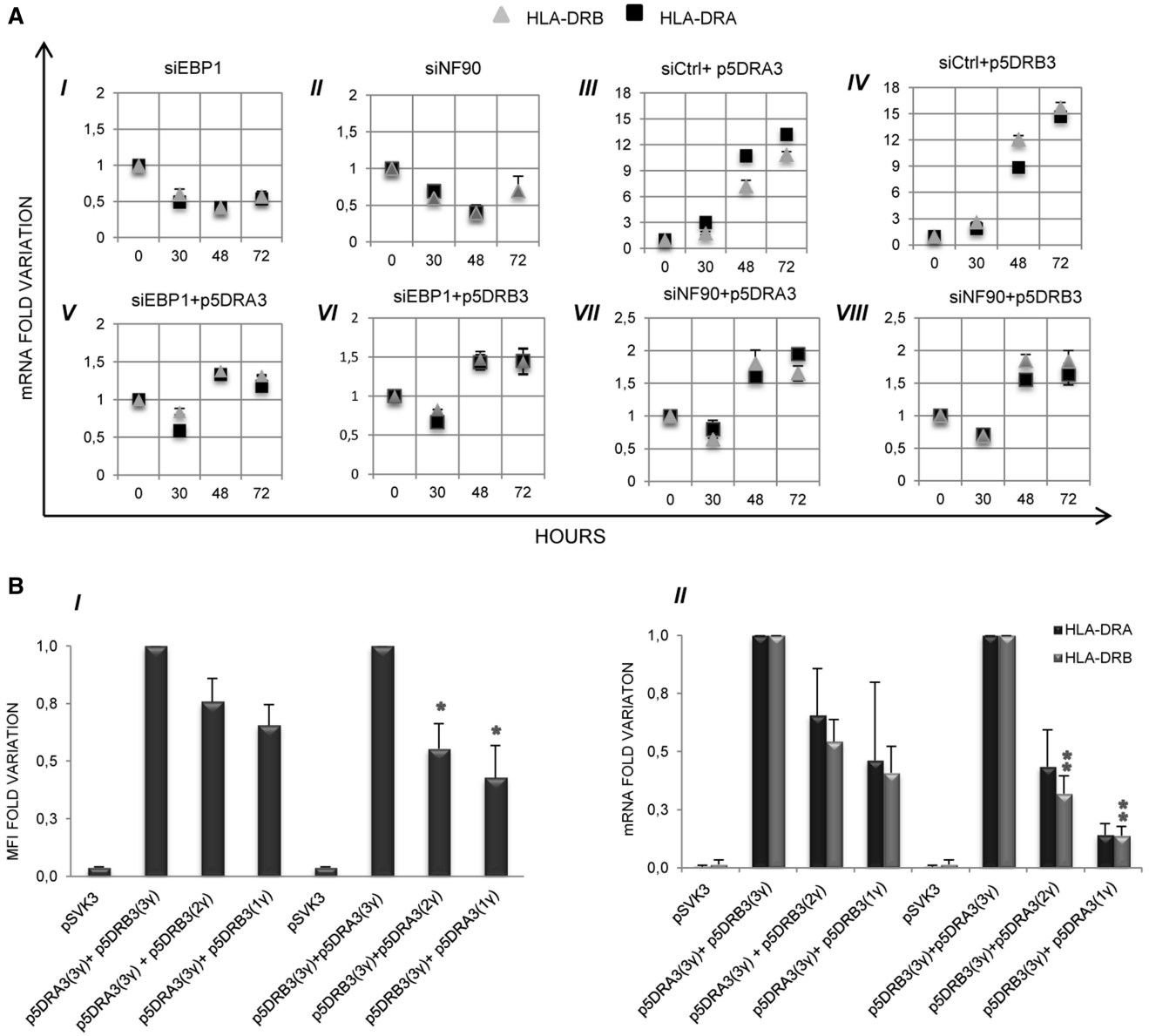

Figure 4. Modulation of MHCII expression. (**A**) The graphs illustrate the time course (0, 30, 48 and 72 h) of DRA and DRB mRNAs fold variation in M14 cells measured by qRT–PCR after 24 h of EBP1 and NF90 proteins silencing and subsequent transfections of indicated plasmids. In details, subpanels show quantification of two messengers after silencing of EBP1 (I) and NF90 (II) and after silencing with siCtrl followed by p5DRA3 (III) and p5DRB3 (IV) transfections. Silencing with siEBP1 followed by p5DRA3 (V) and p5DRB3 (VI) transfections, and knockdown with siNF90 followed by p5DRA3 (VII) and p5DRB3 (VIII) transfections were shown. (**B**) (I) Cytofluorimetric analysis of HLA-DR surface expression in HeLa cells 48 h after transfection with indicated amount of pSVK3, p5DRA3 and p5DRB3 reported as fold change of MFI. (II) DRA and DRB mRNAs variation measured by qRT–PCR in cells were analysed in the same experimental conditions. In the case of DRB mRNA, *P*-value is calculated with respect to the maximum amount of p5DRA3 used; for DRA mRNA, *P*-value is calculated with respect to the maximum amount of p5DRB3 transfected.

were carried out using S100 extracts from both Raji (data not shown) and M14 cell lines (Figure 5), and results showed a clear interaction between cytoplasmic proteins and 5DRA (A, lane 3) and 5DRB (B, lane 3) riboprobes. In addition, we performed competition experiments between the 5′- and 3′-UTR proper or of the other chain; as shown in A, the binding to 5DRA riboprobe was completely displaced by 3DRA (lanes 7–9), and with lesser extent by 5DRB (lanes 4–6) and 3DRB (lanes 10–12) cold riboprobes. Panel B shows that the cytoplasmic proteins interaction with 5DRB was displaced by 3DRA (lanes 10–12), 5DRA (lanes 4–6) and 3DRB (lanes 7–9) cold riboprobes in a similar manner. This experiment allows us to conclude that 5′-UTRs are able to interact with the same proteins if incubated with cytoplasmic extracts, although with different affinity. Moreover, we observed that the 3′-UTR of the DRA chain is always the strongest competitor, suggesting a prevalent role of this chain, according to the analysis of stability (Figure 3) and data obtained in HeLa cells (Figure 4B).

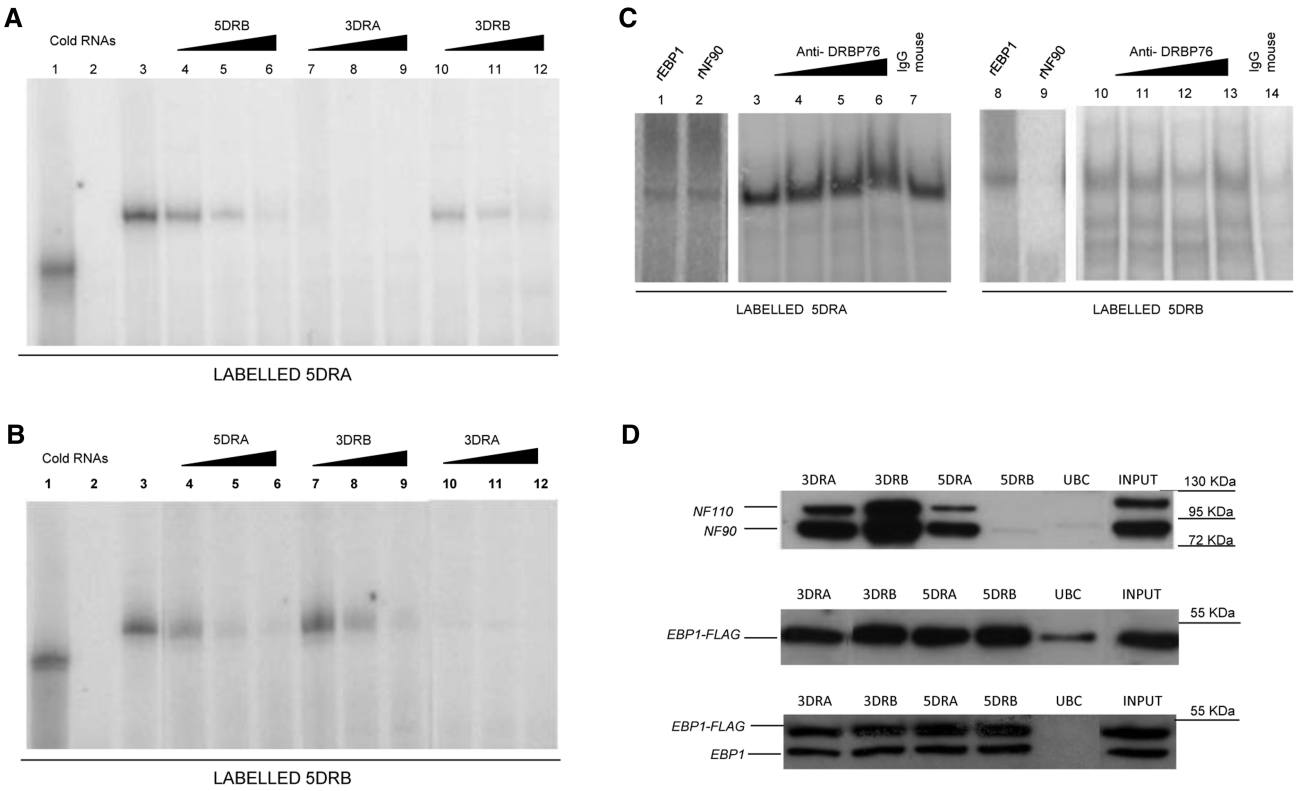

Figure 5. Analysis of interactions of MHCII RNP components. (**A**) REMSAs experiments performed using 5DRA (lane 1) riboprobe; lane 2 shows the digestion with T1 RNase. Lane 3 shows the band of interaction of M14 extract with 5DRA. Competition experiments of 5DRA binding were performed using 0.5, 1 and 2.5 μg of cold 5DRB (lanes 4–6), 3DRA (lanes 7–9) and 3DRB (lanes 10–12). (**B**) REMSAs experiments performed using 5DRB (lane 1) riboprobe; lane 2 shows the digestion with T1 RNase. Lane 3 shows band of interaction of M14 extract with 5DRB. Competition experiments of 5DRB binding were performed using 0.5, 1 and 2.5 μg of cold 5DRA (lanes 4–6), 3DRB (lanes 7–9) and 3DRA (lanes 10–12). (**C**) REMSAs experiments performed using 5DRA (on the left) and 5DRB (on the right) riboprobes. Lane 1 shows the interaction with rEBP1, lane 2 with rNF90 and lane 3 shows band of binding with M14 extract, whereas lanes 4–6 show the supershift of cytoplasmic complex with anti-DRBP76 in binding reaction containing 0.25, 1.25 and 2.5 μg of anti-DRBP76 antibody. No supershift was evident in the presence of 2.5 μg of control IgG (lane 7). Lane 8 shows the interaction of 5DRB with rEBP1, lane 9 demonstrates the absence of binding with rNF90, lanes 10 shows band of interaction of M14 extract, whereas no supershift of cytoplasmic complex with anti-DRBP76 was found in binding reaction containing 0.25, 1.25 and 2.5 μg of anti-DRBP76 antibody (lanes 11–13), similar to that observed in the presence of 2.5 μg of control IgG (lane 14). (**D**) Western blot analysis of biotin pull-down assay carried by using 5DRA, 5DRB, 3DRA, 3DRB and UBC biotinylated riboprobes, after incubation whit cytoplasmic lysate from M14 cells. The top panel represents the immunoblot performed by anti-NF90, whereas the middle and the bottom panels correspond to the western carried out by anti-FLAG and anti-EBP1, respectively, able to detect EBP1 protein. Molecular weights are indicated.

Then we moved to verify the binding of EBP1 and NF90 proteins to 5DRA and 5DRB by performing REMSA with recombinant proteins. The results reported in Figure 5C show that only 5DRA interacts with both proteins (lanes 1 and 2), whereas 5DRB interacts with rEBP1 but does not bind rNF90 (lanes 7 and 8). The supershift assays performed with an anti-DRBP76 antibody confirmed retardation in the mobility of 5DRA (lanes 4–6) but not of 5DRB (lanes 11–13) with cytoplasmic proteins, indicating the exclusion of 5DRB from binding to NF90 in the RNP complex.

To further validate the interaction of EBP1 and NF90 to 5′- and 3′-UTRs riboprobes, we performed a biotin pull-down assay (Figure 5D). *In vitro* transcribed biotinylated 5DRA, 5DRB, 3DRA, 3DRB and UBC (used as negative control) were incubated with M14 cytoplasmic proteins. After pull-down with streptavidin-coated beads, proteins interacting with biotinylated riboprobes were detected by western blot. The anti-DRBP76 antibody revealed the presence of both NF90 and NF110 isoforms (upper panel) in the samples precipitated by 5DRA, 3DRA and 3DRB, but not in samples precipitated with 5DRB. The same biotinylated riboprobes were incubated with cytoplasmic protein lysates from stable transfected M14–EBP1–FLAG cells, and the interaction with specific protein was revealed by anti-FLAG (middle panel) and anti-EBP1 antibodies (lower panel), demonstrating the binding of all UTRs to EBP1. The pull-down assay confirmed the direct interaction of UTRs MHCII with EBP1 and NF90 proteins, except the binding of 5DRB to NF90. In conclusion, beyond the previously identified 3′-UTRs, we confirmed the inclusion of 5′-UTRs as *cis* elements of the MHCII RNA operon, interacting with EBP1, NF90 and other not yet identified protein factors.

Common motifs were found in the UTRs of DRA and DRB mRNAs

We performed a computational analysis of 5′- and 3′-UTRs of DRA and DRB mRNAs to find any common

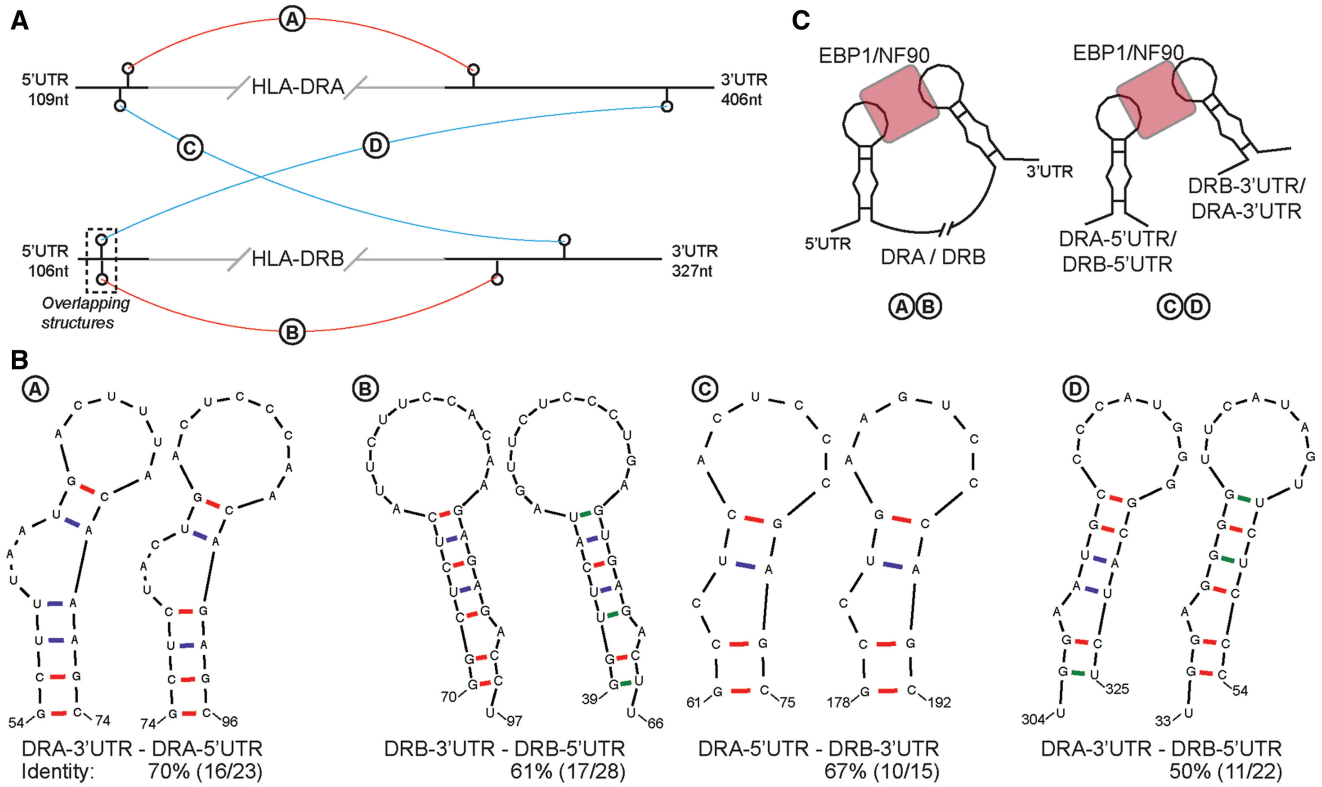

Figure 6. RNA secondary structure motifs. (**A**) Locations of the common secondary structure motifs between the 5′- and 3′-UTRs of the same RNA to form an enclosed loop [(A) HLA-DRA and (C) HLA-DRB] and between the two different RNAs to form a heterogenic complex [(C) DRA-5′-UTR to DRB-3′-UTR and (D) DRB-5′-UTR to DRA-3′-UTR]. In the HLA-DRB 5′-UTR, there are two overlapping structures that are unlikely to be able to co-exist; therefore, only one at any one time can act as a *cis*-acting signal. (**B**) The individual RNA secondary structure motifs arranged in matching pairs. Each motif is locally stable and with a >50% sequence identity. (**C**) Possible binding modes between the common secondary structure motifs within the RNP containing EBP1 and NF90. The binding modes are between the 5′- and 3′-UTR of the same RNA molecule and between the UTRs of different RNAs.

sequence and/or structural features within the RNAs. A FOLDALIGN analysis against all pairs of sequences revealed common sequence/secondary structure motifs consistent with functional bridge formation (Figure 6A). Each structure is locally stable, enhancing the likelihood of their presence *in vivo*. Common motifs were found in DRA between the 5′- and 3′-UTR, within DRB between the 5′- and 3′-UTR, between 5DRA and 3DRB and between 5DRB and 3DRA (Figure 6B). Each single protein binds one or more motifs, generating functional bridges either within one RNA or across two different RNAs (Figure 6C). The common motifs allow two types of interactions to take place, first between 5′- and 3′-UTR of the same RNA to form an enclosed loop structure (Figure 6C left), and second interactions across UTRs of different RNAs to form a heterogeneous complex within the RNP (Figure 6C right). In the 5′-UTR of DRB, the two predicted structures with major similarity were overlapping (Figure 6A); therefore, they are unlikely to co-exist at the same time, and for this reason, 5DRB seems to be less locally stable than the other motifs predicted, providing a possible explanation for the absence of NF90 binding. The choice of formed structures in the cases of overlap is likely to be dependent on the affinity or the relative concentrations of the RNA-binding proteins present. The formation of functional bridges between the UTRs of DRA and DRB is likely to be dependent on common RNA secondary structure motifs interacting with the RNA binding domains of the protein components of the 'RNA operon'.

RNP complex links α and β chains together

To test how NF90 and EBP1 are able to interconnect 5′- and 3′-UTRs, we performed a 5′–3′ co-precipitation experiment. The 3′-UTR ^{32}P-labelled riboprobes were precipitated using biotin-labelled 5′-UTR riboprobes in presence of 0.1, 0.2, 0.4, 0.8 and 1 μg of rNF90 or rEBP1 and 1 μg BSA. Specifically, streptavidin-beads covered with biotinylated 5DRA or 5DRB were incubated with ^{32}P-3DRA or ^{32}P-3DRB, previously incubated with increasing amount of recombinant proteins. In Figure 7, we observed that 3DRA riboprobe was clearly precipitated by 5DRA in presence of rNF90 and rEBP1 compared with BSA (A); otherwise 3DRA was precipitated by 5DRB riboprobe only in presence of rEBP1 (B).

In addition, 3DRB riboprobe was precipitated by 5DRA (C) in presence of both proteins, whereas it was precipitated by 5DRB (D) only in presence of rEBP1. These data demonstrated that rEBP1 and rNF90 bind simultaneously both the UTRs of the same DRA and

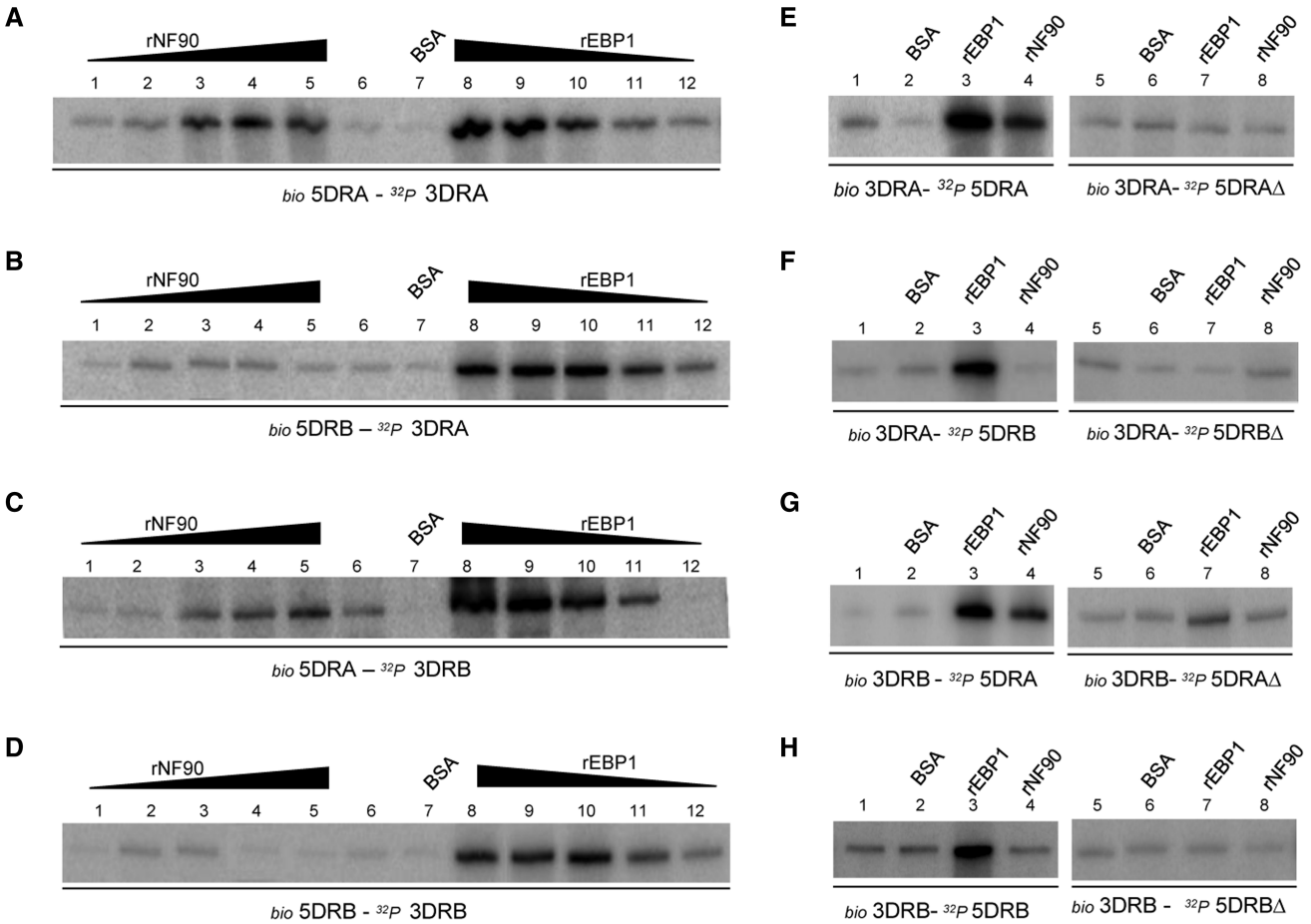

Figure 7. The 5′–3′ co-precipitation assay. All experiments were performed by biotinylated riboprobes, indicated with *bio* prefix, and ^{32}P-UTP–labelled riboprobes indicated with ^{32}P prefix. (**A–D**) Experiments carried out in presence of indicated biotinylated and ^{32}P-riboprobes and 0.1, 0.2, 0.4, 0.8 and 1 μg rNF90 (lanes 1–5), no protein (lanes 6), 1 μg BSA (lane 7) and 1, 0.8, 0.4, 0.2 and 0.1 μg rEBP1 (lanes 8–12). (**E–H**) Experiments carried out in presence of indicated biotinylated and ^{32}P-riboprobes without protein (lanes 1 and 5), in presence of 1 μg of BSA (lane 2 and 6), 1 μg rEBP1 (lanes 3 and 7) and 1 μg rNF90 (lanes 4 and 8).

DRB messenger and join 5′- and 3′-UTR of different transcripts, with exception of 5DRB/NF90 interaction.

To further validate the specificity of this interaction and also to verify whether the stem–loop predicted structures identified by the computational analysis determine the *intra*- and *inter*- chains binding trough NF90 and EBP1, we performed another co-precipitation assay using a reverse labelling of the riboprobes and mutated riboprobes, named 5DRAΔ and 5DRBΔ. We deleted 40 and 50 bases of 5DRA and 5DRB, respectively (see sequences in Supplementary Table S3), necessary to form the predicted stem–loop structures. In this experiment, the 5′-UTR or the 5′-UTRΔ ^{32}P-labelled riboprobes were precipitated using biotin-labelled 3′-UTR riboprobes in presence of 1 μg of rNF90, rEBP1 and BSA. We observed that ^{32}P-5DRA was precipitated by biotinylated 3DRA or 3DRB in presence of rEBP1 and rNF90 (E and G), whereas ^{32}P-5DRB was precipitated by biotinylated 3DRA or 3DRB only in presence of rEBP1 (F and H), confirming previous results, whereas both ^{32}P-5DRAΔ and ^{32}P-5DRBΔ were always unable to precipitate biotin-labelled 3DRA and 3DRB riboprobes in presence of any recombinant proteins (E–H) compared with full-length riboprobes.

The 5′–3′ co-precipitation assays confirm that rEBP1 binds both UTRs of DRA and DRB mRNAs and links 3′-UTR of a messenger with 5′-UTR of the other transcript. Differently, rNF90 interacts with both terminus of DRA and allows only the binding of 5DRA with 3DRB. These data suggest that EBP1 and NF90 are involved in the establishment of functional bridges inside the RNP complex by connecting 5′- and 3′-UTRs (see model in Figure 8).

DISCUSSION

Gene expression is a coordinated process that comprises different linked steps, such as transcription, RNA processing, nucleus–cytoplasm export, translation and degradation of mRNAs. *Trans*-acting factors, interacting with 5′-UTRs and 3′-UTRs of messengers coordinate these processes inside the post-transcriptional operon (18). Many studies support the functional integration of transcription to the splicing, to the 3′-end processing (19,20)

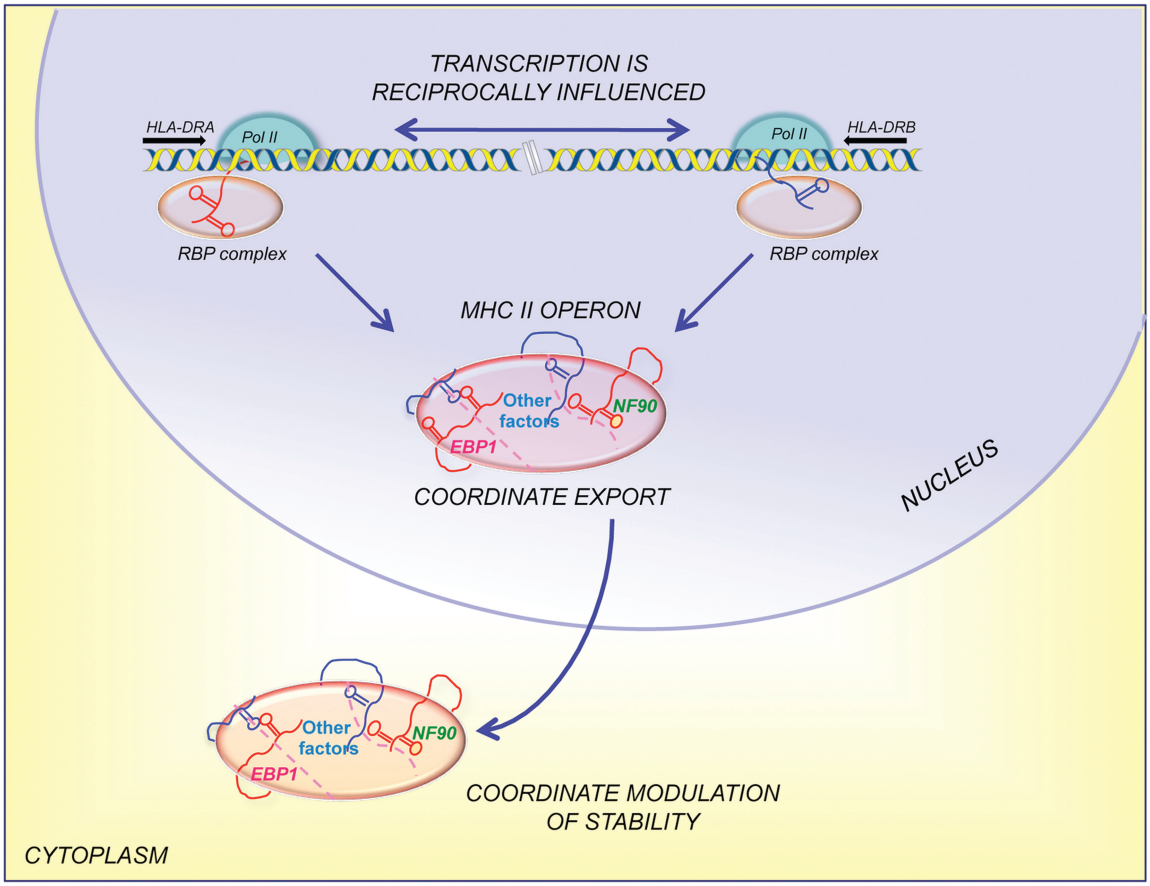

Figure 8. MHC II RNA operon bridging model. RNP complex binds 5′- and 3′-UTR of the DRA and DRB mRNAs and links 3′-UTR of a messenger with 5′-UTR of the other transcript. This bridging model interplays transcription with RNA processing inside the nucleus and in the cytoplasm.

and to mRNA export (21). The interplay among transcriptional control and mRNA stability directs the temporal order of induction of genes encoding inflammatory molecules (22), whereas temporally coordinated changes in populations of HuR associated mRNAs occur during T-cell activation (23).

Our work investigated the fate of mRNAs encoding polypeptides forming MHCII surface heterodimers belonging to the HLA-DQ and HLA-DR isotypes. In this context, we were interested in the open question regarding the stoichiometric balance of the two mRNAs that will encode MHCII heterodimeric molecules. We know that the transcription of DRA and DRB polymorphic genes is strictly coordinated, but there is a lack of available data about the events downstream of the transcription. To unravel this issue, we perturbed the existing equilibrium state between two transcripts by the ectopic expression of a full-length messenger encoding DR α or β chain, and we observed an increase in the amount of endogenous mRNAs encoding for the other chain. This phenomenon, referred as 'co-regulation', occurred in both professional APCs, a Raji B lymphoma cell line and primary monocytes, as well as in non-professional APCs, as M14 cell lines, also for the DQ isotype. We describe here, for the first time, a kind of balance that has to be maintained between two transcripts whose proteins have to be assembled in a heterodimeric surface molecule, in several cell types. The *cis* elements responsible for this co-regulation are the 5′- and 3′-UTRs because transfections performed with cDNA deleted of these regions fail to induce a clear increase of endogenous-related transcript, also because of the lower amount of ectopic mRNA produced. Transfections, with chimeric constructs carrying GFP coding region fused to 5′- and/or 3′-UTR of DRA, allow us to confirm the role of these regulatory regions that, when provided in *trans* by a non-related transcript, were able to stimulate the increase of both endogenous DRA and DRB mRNAs; the UTR regions are the key regulators of equilibrium being able *per se* to induce variation of their messengers.

To better evaluate the co-regulation, we individually analysed transcription, export and stability of DRA and DRB mRNA. By ChIP assay, we have shown an increase of DRA transcription after the ectopic expression of full-length DRB, which is not observed using the construct deleted of 3′-UTR. This result shows a function of 3′-UTR on the stimulation of Pol II activity at the DRA promoter level, probably mediated by a positive feedback on the transcriptional machinery.

The analysis of cytoplasmic and nuclear mRNA after transfections demonstrated a coordinated export of both endogenous and the exogenous DRA and DRB mRNAs.

In addition, we observed that the depletion of 3′- or 5′-UTR augments the ratio of C/N mRNAs, indicating an increase of the export out of the nucleus already demonstrated in a previous article by the authors (17).

Concerning the modulation of the stability, we observed that after ectopic expression of a full-length construct, there is an increase in half-life of the endogenous messenger encoding the related chain. This increase of stability is also observed in GFP chimeric constructs in which 5DRA and 3DRA influence in *cis* the decay of the exogenous messenger and in *trans* the stability of endogenous DRB transcript. The role of 5′- and 3′-UTR in the half-life modulation seems to be equivalent and synergistic because we have observed an intermediate effect on stability by the chimeric construct carrying only one UTR.

These results clearly demonstrate that the co-regulation occurs at different levels of mRNA processing and can be accomplished thanks to the interaction of UTRs with the RNA-binding protein complex, of which we have identified two factors: EBP1 and NF90 (7). NF90 protein, included in the NFARs family, activates transcription of interleukin-2 (IL-2) (10) and IL-13 (24) and controls the stability and/or export of a wide variety of RNAs (25), functioning as translational sentinels to detect viral RNAs and impede their transcription and translation (26). EBP1, identified as ErbB3-binding protein, is a pleiotropic protein, acting as transcriptional repressor on E2F1 consensus promoters and as RNA-binding protein with the role of stability modulator (9,27). Both proteins are widely described as RNA-binding proteins, with NF90 able to recognize dsRNA, especially targeting A/U rich regions of UTRs (28), and EBP1 capable to preferentially bind structured regions of RNA within RNA complexes (29,30). Moreover, the function of suppressor or/and oncogene described for EBP1 (12,31) allows us to hypothesize a relationship between cancer and MHCII-mediated immune response. This aspect becomes especially relevant if we consider that in non-professional APCs, such as cancer cells, the surface expression of MHCII could consent epitope cancer presentation and subsequent CD4 immune response to the tumour.

In our system, the depletion of EBP1 and NF90 by siRNA transfection, inhibits the overexpression of both ectopic and endogenous MHCII mRNAs, indicating the fundamental role of these proteins on the modulation of MHCII expression. Pull-down experiments demonstrate the direct binding of EBP1 to the 3′-UTR and to 5′-UTR of both DRA and DRB mRNAs and the interaction of NF90 with 5DRA, 3DRA and 3DRB, but not with 5DRB. This result could be related to other data concerning DRB messenger: the transfection of constant amount of a plasmid encoding one mRNA and a variable quantity of the plasmid encoding the other transcript in HeLa cells, demonstrates, in fact, not only that the co-regulation takes place also in cells negative for MHCII expression but also that the heterodimer surface density is essentially modulated by DRA mRNA amount and to a minor extent by DRB mRNA quantity. The higher stability of the DRA transcript, the greater affinity of its UTRs for the protein complex and also the absence of polymorphism with respect to other MHC II mRNAs, suggests that the main role of this messenger in the operon context is to establish the balance with its cognate mRNA.

As reported in the literature, EBP1 is theoretically capable of binding two separate RNA structured regions, although it is yet to be observed *in vivo* (32), whereas the formation of a loop structure has been already demonstrated for NF90 associating with both termini of a viral RNA genome, structure important for the coordination of translation and replication (33). On this basis, by a 5′/3′ co-precipitation assay, we found that rEBP1, at the same time, interacts with 5′- and 3′-ends inside each DRA or DRB transcripts and links 5DRA to 3DRB and 5DRB to 3DRA. Differently, rNF90 fails in all the interactions involving 5DRB, according to REMSA and pull-down assays, whereas it is able to interconnect 5DRA to its proper 3DRA and to 3DRB. The specificity of this interaction is validated by mutagenesis, as 5′-UTRs carrying 40–50 nt deletions were unable to keep the interactions with 3′-UTR.

The mutual relationships inside RNP can be related to the computational analysis of the RNA secondary structures that have identified similar motifs in all UTRs of DRA and DRB. The sequence identity of these motifs is >50%, supporting the building of a loop conformation of two mRNAs through several RNA-binding proteins, giving, in particular, a possible explanation of the recognition of several UTRs by EBP1 and NF90.

RNA-binding proteins, in fact, often comprise multiple RNA-binding domains building up specificity and affinity by binding multiple short sites (4–8 nt) on the RNA, and many RNA-binding domains are also functional as protein:protein interaction sites (34), such as NF90 (35), although its tissue-specific isoforms have made the elucidation of RNA target motifs an area of controversy (36). The RNA secondary structure prediction of the entire mRNA is not likely to be consistent with the *in vivo* structure; however, the local environment around a potential binding site determines the accessibility and stability of the motif (37). Furthermore, even if secondary structures are highly dynamic, they are often stabilized on binding to their protein partners (38).

Here, we propose a model in which MHCII RNA operon regulates the stoichiometric balance of the related DRA and DRB messengers, resulting in a balanced assembly of α and β polypeptides to obtain a functional heterodimeric molecule, both for DQ and DR isotypes (Figure 8). This equilibrium is modulated at mRNAs level by a complex mechanism involving the transcription and the downstream steps of the mRNAs processing. According to the operon model, RNAs are decorated with proteins throughout their lifetimes in a highly dynamic structure; we hypothesize that the RNP, comprising not only EBP1 and NF90 but also other as yet unidentified proteins, docks the rising DRA and DRB mRNAs at UTRs level already during transcription, and it joins together the two chains building functional bridges during the proceeding processes. In this context, the alteration of the equilibrium through *in vitro* transfection induces the RNP machinery to restore the previous balance influencing the transcriptional rate of the PolII

complex. Furthermore, the two transcripts are simultaneously regulated both for the nucleus–cytoplasm export and decay in the cytoplasm; in this context, the role of both UTRs is essential, as they contain the recognition sites of *trans*-acting proteins. This scenario has to be extended for its implications; the artificial perturbation we have induced can mimic the cell environmental changes after an activation stimulus. If the cells have to present antigens and, as consequence, a modulation of MHCII expression is required, there is a rapid RNP remodelling that guarantees the coordinate and balanced processing of the two related transcripts.

SUPPLEMENTARY DATA

Supplementary Data are available at NAR Online: Supplementary Tables 1–3, Supplementary Figures 1 and 2 and Supplementary Materials and Methods.

ACKNOWLEDGEMENTS

The authors thank Prof. A. Hamburger for providing the plasmid encoding EBP1 cDNA and the IGB FACS facility.

FUNDING

Funding for open access charge: Italian Ministry of Research [FIRB project n. RBLA033WJX].

Conflict of interest statement. None declared.

REFERENCES

1. Cresswell,P. (1994) Assembly, transport, and function of MHC class II molecules. *Annu. Rev. Immunol.*, **12**, 259–293.
2. Villadangos,J.A., Schnorrer,P. and Wilson,N.S. (2005) Control of MHC class II antigen presentation in dendritic cells: a balance between creative and destructive forces. *Immunol. Rev.*, **207**, 191–205.
3. Viret,C. and Janeway,C.A. Jr (1999) MHC and T cell development. *Rev. Immunogenet.*, **1**, 91–104.
4. Steimle,V., Siegrist,C.A., Mottet,A., Lisowska-Grospierre,B. and Mach,B. (1994) Regulation of MHC class II expression by interferon-gamma mediated by the transactivator gene CIITA. *Science*, **265**, 106–109.
5. Guardiola,J. and Maffei,A. (1993) Control of MHC class II gene expression in autoimmune, infectious, and neoplastic diseases. *Crit. Rev. Immunol.*, **13**, 247–268.
6. Ting,J.P. and Trowsdale,J. (2002) Genetic control of MHC class II expression. *Cell*, **109(Suppl)**, S21–S33.
7. Corso,C., Pisapia,L., Citro,A., Cicatiello,V., Barba,P., Cigliano,L., Abrescia,P., Maffei,A., Manco,G. and Del Pozzo,G. (2011) EBP1 and DRBP76/NF90 binding proteins are included in the major histocompatibility complex class II RNA operon. *Nucleic Acids Res.*, **39**, 7263–7275.
8. Barber,G.N. (2009) The NFAR's (nuclear factors associated with dsRNA): evolutionarily conserved members of the dsRNA binding protein family. *RNA Biol.*, **6**, 35–39.
9. Zhou,H., Mazan-Mamczarz,K., Martindale,J.L., Barker,A., Liu,Z., Gorospe,M., Leedman,P.J., Gartenhaus,R.B., Hamburger,A.W. and Zhang,Y. (2010) Post-transcriptional regulation of androgen receptor mRNA by an ErbB3 binding protein 1 in prostate cancer. *Nucleic Acids Res.*, **38**, 3619–3631.
10. Shi,L., Godfrey,W.R., Lin,J., Zhao,G. and Kao,P.N. (2007) NF90 regulates inducible IL-2 gene expression in T cells. *J. Exp. Med.*, **204**, 971–977.
11. Zhang,Y., Wang,X.W., Jelovac,D., Nakanishi,T., Yu,M.H., Akinmade,D., Goloubeva,O., Ross,D.D., Brodie,A. and Hamburger,A.W. (2005) The ErbB3-binding protein Ebp1 suppresses androgen receptor-mediated gene transcription and tumorigenesis of prostate cancer cells. *Proc. Natl Acad. Sci. USA*, **102**, 9890–9895.
12. Lessor,T.J., Yoo,J.Y., Xia,X., Woodford,N. and Hamburger,A.W. (2000) Ectopic expression of the ErbB-3 binding protein ebp1 inhibits growth and induces differentiation of human breast cancer cell lines. *J. Cell. Physiol.*, **183**, 321–329.
13. Soutoglou,E. and Talianidis,I. (2002) Coordination of PIC assembly and chromatin remodeling during differentiation-induced gene activation. *Science*, **295**, 1901–1904.
14. Livak,K.J. and Schmittgen,T.D. (2001) Analysis of relative gene expression data using real-time quantitative PCR and the 2(-Delta Delta C(T)) Method. *Methods*, **25**, 402–408.
15. Vashist,S., Bhullar,D. and Vrati,S. (2011) La protein can simultaneously bind to both 3'- and 5'-noncoding regions of Japanese encephalitis virus genome. *DNA Cell Biol.*, **30**, 339–346.
16. Havgaard,J.H., Torarinsson,E. and Gorodkin,J. (2007) Fast pairwise structural RNA alignments by pruning of the dynamical programming matrix. *PLoS Comput. Biol.*, **3**, 1896–1908.
17. Del Pozzo,G., Ciullo,M., Autiero,M. and Guardiola,J. (1994) Control of nucleo-cytoplasmic HLA-DRA mRNA partitioning by interaction of a retention signal with compartmentalized proteins. *J. Mol. Biol.*, **240**, 193–204.
18. Keene,J.D. (2007) RNA regulons: coordination of post-transcriptional events. *Nat. Rev. Genet.*, **8**, 533–543.
19. Mapendano,C.K., Lykke-Andersen,S., Kjems,J., Bertrand,E. and Jensen,T.H. (2010) Crosstalk between mRNA 3' end processing and transcription initiation. *Mol. Cell*, **40**, 410–422.
20. Nagaike,T., Logan,C., Hotta,I., Rozenblatt-Rosen,O., Meyerson,M. and Manley,J.L. (2011) Transcriptional activators enhance polyadenylation of mRNA precursors. *Mol. Cell*, **41**, 409–418.
21. Garcia-Oliver,E., Garcia-Molinero,V. and Rodriguez-Navarro,S. (2012) mRNA export and gene expression: The SAGA-TREX-2 connection. *Biochim. Biophys. Acta*, **1819**, 555–565.
22. Hao,S. and Baltimore,D. (2009) The stability of mRNA influences the temporal order of the induction of genes encoding inflammatory molecules. *Nat. Immunol.*, **10**, 281–288.
23. Mukherjee,N., Lager,P.J., Friedersdorf,M.B., Thompson,M.A. and Keene,J.D. (2009) Coordinated posttranscriptional mRNA population dynamics during T-cell activation. *Mol. Syst. Biol.*, **5**, 288.
24. Kiesler,P., Haynes,P.A., Shi,L., Kao,P.N., Wysocki,V.H. and Vercelli,D. (2010) NF45 and NF90 regulate HS4-dependent interleukin-13 transcription in T cells. *J. Biol. Chem.*, **285**, 8256–8267.
25. Vumbaca,F., Phoenix,K.N., Rodriguez-Pinto,D., Han,D.K. and Claffey,K.P. (2008) Double-stranded RNA-binding protein regulates vascular endothelial growth factor mRNA stability, translation, and breast cancer angiogenesis. *Mol. Cell. Biol.*, **28**, 772–783.
26. Pfeifer,I., Elsby,R., Fernandez,M., Faria,P.A., Nussenzveig,D.R., Lossos,I.S., Fontoura,B.M., Martin,W.D. and Barber,G.N. (2008) NFAR-1 and -2 modulate translation and are required for efficient host defense. *Proc. Natl Acad. Sci. USA*, **105**, 4173–4178.
27. Zhang,Y., Woodford,N., Xia,X. and Hamburger,A.W. (2003) Repression of E2F1-mediated transcription by the ErbB3 binding protein Ebp1 involves histone deacetylases. *Nucleic Acids Res.*, **31**, 2168–2177.
28. Kuwano,Y., Pullmann,R. Jr, Marasa,B.S., Abdelmohsen,K., Lee,E.K., Yang,X., Martindale,J.L., Zhan,M. and Gorospe,M. (2010) NF90 selectively represses the translation of target mRNAs bearing an AU-rich signature motif. *Nucleic Acids Res.*, **38**, 225–238.
29. Bose,S.K., Sengupta,T.K., Bandyopadhyay,S. and Spicer,E.K. (2006) Identification of Ebp1 as a component of cytoplasmic bcl-2 mRNP (messenger ribonucleoprotein particle) complexes. *Biochem. J.*, **396**, 99–107.

30. Squatrito,M., Mancino,M., Sala,L. and Draetta,G.F. (2006) Ebp1 is a dsRNA-binding protein associated with ribosomes that modulates eIF2alpha phosphorylation. *Biochem. Biophys. Res. Commun.*, **344**, 859–868.
31. Kim,C.K., Nguyen,T.L., Joo,K.M., Nam,D.H., Park,J., Lee,K.H., Cho,S.W. and Ahn,J.Y. (2010) Negative regulation of p53 by the long isoform of ErbB3 binding protein Ebp1 in brain tumors. *Cancer Res.*, **70**, 9730–9741.
32. Kowalinski,E., Bange,G., Bradatsch,B., Hurt,E., Wild,K. and Sinning,I. (2007) The crystal structure of Ebp1 reveals a methionine aminopeptidase fold as binding platform for multiple interactions. *FEBS Lett.*, **581**, 4450–4454.
33. Isken,O., Grassmann,C.W., Sarisky,R.T., Kann,M., Zhang,S., Grosse,F., Kao,P.N. and Behrens,S.E. (2003) Members of the NF90/NFAR protein group are involved in the life cycle of a positive-strand RNA virus. *EMBO J.*, **22**, 5655–5665.
34. Lunde,B.M., Moore,C. and Varani,G. (2007) RNA-binding proteins: modular design for efficient function. *Nat. Rev. Mol. Cell. Biol.*, **8**, 479–490.
35. Parrott,A.M., Walsh,M.R. and Mathews,M.B. (2007) Analysis of RNA:protein interactions in vivo: identification of RNA-binding partners of nuclear factor 90. *Methods Enzymol.*, **429**, 243–260.
36. Neplioueva,V., Dobrikova,E.Y., Mukherjee,N., Keene,J.D. and Gromeier,M. (2010) Tissue type-specific expression of the dsRNA-binding protein 76 and genome-wide elucidation of its target mRNAs. *PLoS One*, **5**, e11710.
37. Lange,S.J., Maticzka,D., Mohl,M., Gagnon,J.N., Brown,C.M. and Backofen,R. (2012) Global or local? Predicting secondary structure and accessibility in mRNAs. *Nucleic Acids Res.*, **40**, 5215–5226.
38. Doetsch,M., Schroeder,R. and Furtig,B. (2011) Transient RNA-protein interactions in RNA folding. *FEBS J.*, **278**, 1634–1642.